Pulse Radiolysis of Supercritical Water. 3. Spectrum and Thermodynamics of the Hydrated Electron

ARTICLE *in* THE JOURNAL OF PHYSICAL CHEMISTRY A · MARCH 2005

Impact Factor: 2.69 · DOI: 10.1021/jp0457141 · Source: PubMed

Pulse Radiolysis of Supercritical Water. 3. Spectrum and Thermodynamics of the Hydrated Electron

David M. Bartels*

Notre Dame Radiation Laboratory, Notre Dame, Indiana 46556

Kenji Takahashi,† Jason A. Cline,‡ Timothy W. Marin,§ and Charles D. Jonah

Chemistry Division, Argonne National Laboratory, Argonne, Illinois 60439

Received: September 21, 2004; In Final Form: October 29, 2004

Spectra of the hydrated electron in pressurized light and heavy water at temperatures up to and beyond the critical temperature are reported, for wavelengths between 0.4 and 1.7 μm. In agreement with previous work, spectra can be approximately represented by a Gaussian function on the low-energy side, and a Lorentzian function on the high-energy side in subcritical water, but deviations from this form are very clear above 200 °C. The spectrum shifts strongly to the red as temperature rises. At supercritical temperatures, the spectrum shifts slightly to the red as density decreases, and the Gaussian−Lorentzian form is a very poor description. Application of spectral moment theory allows one to make an estimate of the average size of the electron wave function and of its kinetic energy. It appears that for water densities below about 0.6 g/cc, and down to below 0.1 g/cc, the average radius of gyration for the electron remains constant at around 3.4 Å, and its absorption maximum is near 0.9 eV. For higher densities, the electron is squeezed into a smaller cavity and the spectrum is shifted to the blue. The enthalpy and free energy of electron hydration are derived as a function of temperature on the basis of existing equilibrium data and absolute proton hydration energies derived from the cluster-based common point method. In a discussion, we compare the effective "size" of the hydrated electron derived from both methods.

Introduction

Technological interest continues to be great in the use of supercritical water as an environmentally friendly "green" reaction medium for destruction of hazardous waste and even some synthesis schemes.[1−3] It is little appreciated that supercritical water is already commonly used as the heat transfer medium in modern high-temperature electrical power plants. It has been proposed that this technology should also be extended to new nuclear power plants, but the issue of water radiolysis and radiation-induced corrosion must be addressed. Hydrated electrons are of great importance in the radiation-induced chemistry at all temperatures[4−6] and are also easy to detect because of their intense absorption in the red and near-IR spectral regions. In the first paper of this series we reported the unusual reaction rates of radiation-generated hydrated electrons with hydrophobic solutes O_2 and SF_6.[7] In a second contribution, the diffusion-limited reaction of electrons with nitrobenzene was reported.[8] In this paper we present our detailed measurements of the hydrated electron spectrum at temperatures up to 400 °C in both light and heavy water, and as a function of density (pressure) in the supercritical heavy water at 375 °C. The spectra can be integrated to infer ground-state energetic properties that can ultimately be correlated with reaction rates.

The intense optical absorption spectrum of the hydrated electron has been an object of great theoretical interest since its discovery.[9] The maximum absorption shifts strongly to the red as temperature is raised, from 720 nm at room temperature to ca. 1200 nm at 300 °C.[10] Its shape (plotted in energy units) has been well described by a Gaussian function on the low-energy side, and a Lorentzian function on the high-energy side.[11,12] For many years a debate raged over the bound to bound or bound to continuum nature of the spectrum. Only in recent years, with the advent of large-scale molecular dynamics modeling[13−17] and femtosecond laser probes of the photophysics,[18−21] has the spectrum been unraveled to some extent. There is now no question that near the 720 nm maximum absorption at room temperature, the transition is primarily from bound state to bound state with an "s-to-p-like" transition character.[20] At 400 nm, recent experiments have demonstrated the transition is from bound state to continuum state.[21] The full wavelength and temperature dependence of this bound to bound vs bound to continuum character remains to be fully explored.

In the absence of detailed information of the final state(s) of this transition, the spectrum has nevertheless yielded valuable information about the ground state by way of its moment integrals.[22−26] According to the moment analysis, the $M(-1)$, $M(0)$, and $M(1)$ moments of the spectrum $\gamma(\omega)$ can be characterized with the following relationships (in atomic units):

$$M(-1) = n_0\int_0^\infty \omega^{-1}\gamma(\omega)\,d\omega = \frac{2}{3}\langle r^2\rangle$$

$$M(0) = n_0\int_0^\infty \gamma(\omega)\,d\omega = 1$$

$$M(+1) = n_0\int_0^\infty \omega\gamma(\omega)\,d\omega = \frac{4}{3}\langle T\rangle \qquad (1)$$

$\langle r^2\rangle = \langle |r_{av} - r|^2\rangle$ is the thermally averaged dispersion in position

* To whom correspondence should be addressed. E-mail: bartels@hertz.rad.nd.edu.

† Present address: Department of Chemistry and Chemical Engineering, Kanazawa University, 2-40-20 Kodatsuno, Kanazawa 920-8667, Japan.

‡ Present address: Spectral Sciences, Inc., 4 Fourth Ave., Burlington, MA 01803.

§ Present address: Benedictine University, Department of Chemistry, 5700 College Road, Lisle, IL 60532.

10.1021/jp0457141 CCC: $30.25
Published on Web 01/27/2005

or (squared) radius of gyration for the electron about its average position, n_0 is the refractive index of the medium, and $\langle T \rangle$ is the corresponding kinetic energy. The formulas are derived from dispersion relationships (Kramers−Kronig relations, *f* sum rules) or by analogy to atomic systems using a 1-electron representation. Although the sum rules are rigorous, application of these formulas to solvated electrons depends on two unproven assumptions. First, the coupling of the electron to other electronic degrees of freedom must be sufficiently weak so that oscillator strength is not significantly transferred to or from the solvent spectrum. Second, the corrected local field at the electron is simply the vacuum optical field divided by n_0. Both assumptions seem to work very well for a wide range of solvated electron systems.[22,26,27]

The implication of these formulas is that the spectrum will provide a direct measurement of the average "size" and energy of the electron, which must be changing substantially as a function of temperature. This information should be valuable in understanding the structure, thermodynamics, and reactions of the hydrated electron as a function of temperature. Thermochemical information on the conventional enthalpy and free energy of electrons in water is available up to 250 °C.[28] These numbers are useful in predicting reaction rates, but because they are based on the proton convention ($\Delta X_f^\circ = 0$; $X = H, G, S$), they tell us little about the electron solvation structure. Recently, a new method based on water cluster energetics was introduced for obtaining the absolute hydration thermodynamics for the proton (and all other ions), independent of extrathermodynamic assumptions.[12,29,30] This method has now been applied to obtain thermodynamic information for classical ions over a wide range of temperatures and pressures.[31] In our discussion, the method is extended to obtain absolute solvation thermodynamics of the hydrated electron and the results are compared with the properties deduced from the spectra.

Experimental Section

Hydrated electrons were generated by pulse radiolysis with 20 MeV electrons in a high temperature/pressure flow cell as reported in our previous work.[32,33] Transient absorption signals were recorded with a pulsed xenon lamp/photodiode/transient digitizer combination on time scales from nanoseconds to hundreds of microseconds, depending on the experiment. Wavelengths were selected using (nominally) 12 nm band-pass filters, with band centers ranging from 400 to 1700 nm. The filters were placed in a selector wheel that was rotated by a stepper motor under computer control.

Three different diode detectors have been used in recording spectra, and their properties have been fully described elsewhere.[33] An EG&G FND100 silicon diode was used for some initial spectra from 400 to 1000 nm. A Germanium Power Devices GAP520 InGaAs diode was used to record a number of spectra over the full 400−1700 nm range in heavy water. It was subsequently realized that this diode has a severe wavelength-dependent secondary response characteristic, which makes fitting and reconvolution essential for comparison of different wavelengths. The FND100 diode also suffers from this problem to a lesser extent between 850 and 1000 nm. Our procedure for correcting data and extracting spectra with these detectors is described in detail elsewhere.[33] A third diode used is the Germanium Power Devices GMP566 germanium diode, which we now prefer for most applications. Its speed (55 MHz) is slower than the other diodes mentioned above, but we find a wavelength-independent biexponential response for wavelengths shorter than 1600 nm, and very good quantum efficiency throughout the visible and near-IR. The wavelength-independent response makes measurement of the spectrum much more precise, even though convolutions are required for kinetic data analysis. The response of this diode changes to the red of 1600 nm, and special integration techniques are needed for this spectral region.

It is difficult to normalize the kinetics recorded in our high-temperature/pressure experiments for shot-to-shot variations in the linac pulse, because the all-metal cell construction and connection to pumps defeats practical attempts to integrate the charge/pulse. For most experiments this means that we rely on the linac pulse amplitude and the flowing sample pressure and integrity to be stable over many minutes while spectra are collected, and most often the linac remains stable to the order of 2−3% and pressure fluctuations are on the order of ±0.3 bar. The light water spectra reported below were extracted from experiments in the presence of ca. 0.1 molal H_2 and with pH greater than 11. Under these conditions, all radicals convert to hydrated electrons and a pure second-order decay can be recorded.[34] To confirm the accuracy of the (integrated) spectra, the decay traces at each wavelength were fit from about 2 μs after the radiolysis pulse to obtain the quantity $\epsilon L/2k$, where L is the cell path length, k is the second-order reaction rate constant, and ϵ is the molar extinction coefficient at the probe wavelength. All of these quantities are independent of the applied dose, and only ϵ depends on the wavelength, so the least-squares analysis simultaneously smoothes the data and normalizes for shot-to-shot variations. It was found possible to apply this analysis in light water up to about 300 °C, above which pure second-order decay no longer applies.

To record heavy water spectra, several hundred milliliters of pure 99.5+% D_2O were recirculated with constant argon sparging of the reservoir. The absorption decay near the absorption maximum was first fit to an arbitrary sum of three exponential decay functions. Then the decay shape was held constant and the amplitude of the fitting function was used to determine the spectral intensity at each wavelength. Though we looked carefully, there was no indication of any shift in the spectrum over time that might indicate presence of a second species in the kinetics.

To account for the changing shape of the decay transients due to the secondary response of the GMP566 diode beyond 1600 nm, the entire absorption trace in D_2O was integrated from zero to several microseconds after the electron pulse. On the basis of our previous investigation,[33] the integrated transmittance must be conserved independent of the actual impulse response of the detector. In the limit of small absorbance (optical density < 0.1), the integrated absorbance is also conserved. Consequently, to obtain the infrared points beyond 1600 nm we compared the integrated absorption at those wavelengths with that of two or more wavelengths near the absorption maximum (to the blue of 1600 nm).

A small absorption by the sapphire windows is evident across the entire visible region of the spectrum, where a decay is observed with a time constant >100 μs and an intensity gradually increasing toward shorter wavelengths. In most cases, the window absorption is unobservable at wavelengths ≥ 800 nm, even at the highest radiation doses applied. Because the heavy water hydrated electron absorption decays in <1 μs, the sapphire absorption can be corrected for by adding an additional baseline offset to the fit. The magnitude of the sapphire absorption varied from day to day, depending on the focusing of the linac beam, but typically the hydrated electron absorption

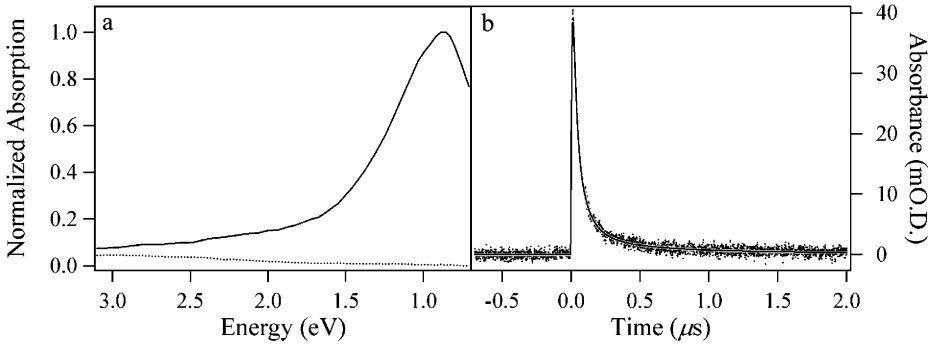

Figure 1. Fitted absorption spectrum for hydrated electron (solid line) and sapphire (dotted line) at 375 °C, 170 bar, density = 0.10 g/cm^3 (a). The electron decay (b, points) in the infrared (near 1 eV) is first fitted to the sum of three arbitrary exponential functions (b, solid line). The sapphire spectrum is a constant baseline offset added to this decay function to correct the kinetics in the visible. This low-density sample represents the very worst case correction for the sapphire window absorbance. In all other cases the 400 nm (3.2 eV) electron absorption is many times larger than the sapphire background.

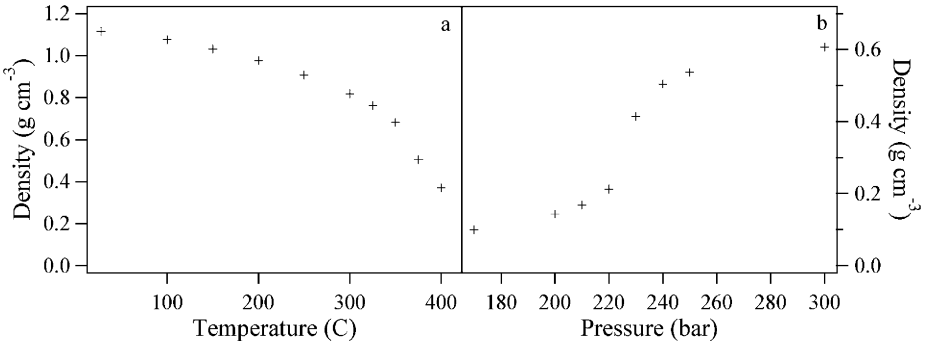

Figure 2. (a) Temperature dependence of the heavy water density at 250 bar, except at 400 °C, where the pressure is 300 bar. (b) Pressure dependence of the heavy water density just above the critical temperature, at 375 °C. Points shown are the actual conditions at which hydrated electron spectra were collected.

intensity at the absorption maximum was ~100 times greater than the intensity of the sapphire absorption at the shortest wavelength (400 nm). The effect of the correction becomes increasingly important for lower water densities, because the intensity of the electron absorption decreases while the sapphire absorption stays constant. Figure 1 shows the fitted absorption spectra for the hydrated electron and sapphire absorption at 375 °C, 170 bar, and density = 0.10 g/cm^3. This is the lowest water density used in these studies, i.e., the worst case where the sapphire absorption is at its maximum relative intensity. A plot of heavy water density vs temperature at 250 bar is illustrated in Figure 2, as well as a plot of the heavy water density vs pressure at 375 °C, just above the critical temperature. These plots reflect the density conditions under which all the presented data were collected.

To calculate densities of light water in this study from the measured temperature and pressure, we use a set of functions based on the IAPWS-IF97 formulation for light water *PVT* relations.[35] Alternatively, water density is supplied by the SUPCRT92 program.[36] The light water dielectric constant is taken from the review by Uematsu and Franck.[37] Heavy water densities are taken from the tabulation and equation of state of Hill et al.[38]

Results

Light water spectra collected in H_2-saturated alkaline solution are shown in Figure 3 as a function of wavelength from 400 to 1350 nm. Care was taken to acquire a large number of points in the visible spectral region to better define the shape of the high-energy side of the spectrum vs energy. All of the points use 12 nm bandwidth filters. The solid lines drawn through the

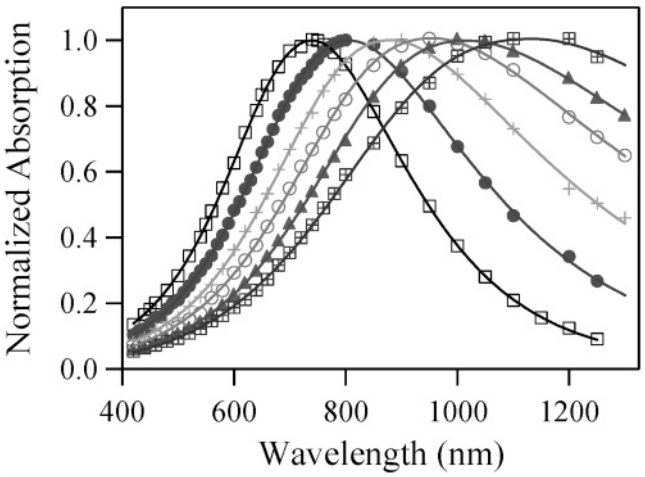

Figure 3. Normalized spectra of the solvated electron in light water at various sub-critical temperatures. Curves are fitted for the modified Gaussian−Lorentzian form in energy, as described in the text. Temperatures for each curve are 46 °C (black, open squares), 100 °C (red, closed circles), 150 °C (orange crosses), 200 °C (green, open circles), 225 °C (blue triangles), and 275 °C (purple, open crossed squares).

points are fitted to a modified Gaussian−Lorentzian form similar to that proposed by Jou and Freeman:[11]

$$\gamma(E) = A_{max} \exp(-[(E - E_{max})/W_r]^2 \ln(2)) \quad \text{for} \quad E < E_{max}$$

$$\gamma(E) = \frac{A_{max}}{1 + [(E - E_{max})/W_b]^Z} \quad \text{for} \quad E > E_{max} \quad (2)$$

where A_{max} is the spectrum intensity at the absorption maximum,

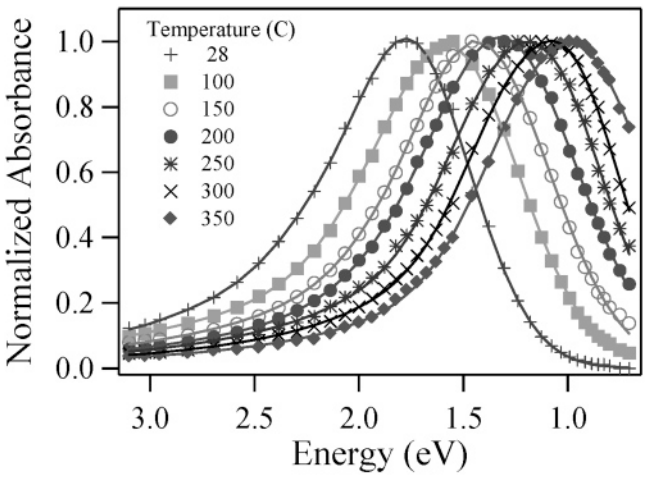

Figure 4. Relative absorption of the hydrated electron in heavy water plotted vs photon energy.

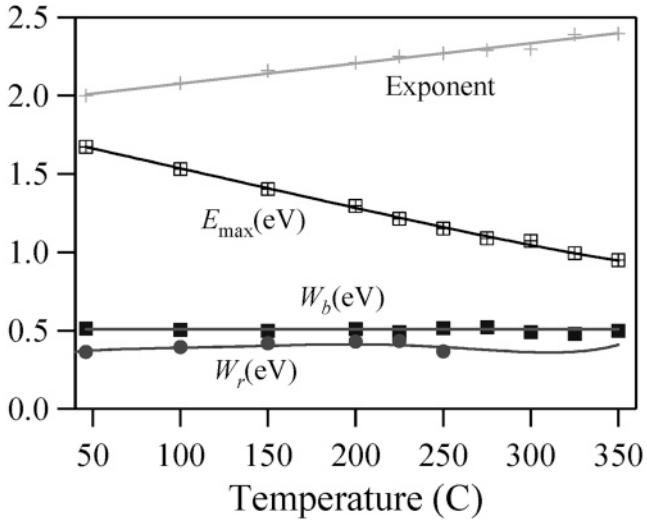

Figure 5. Fitting parameters for the spectra of hydrated electron in light water (symbols) and polynomial fits to the points (smooth lines). Because vibrational overtone absorptions disallow obtaining W_r above 250 °C in light water, the fit to W_r for heavy water is superimposed, extending up to 350 °C.

E_{max} is the energy at the absorption maximum, and W_b and W_r are the half-width at half-maximum of the Lorentzian and Gaussian on the blue and red sides, respectively. Spectra for the hydrated electron in heavy water up to 350 °C are plotted in Figure 4 on an energy scale to illustrate the modified Gaussian−Lorentzian form. Thanks to the lower vibrational frequencies in D_2O, spectra could be recorded out to 1700 nm in the IR. The spectrum in liquid up to 350 °C is essentially independent of the applied pressure to 350 bar. The spectra below 100 °C can be fit very well using an exponent $Z = 2$ on the blue side, just as found by Jou and Freeman.[11] However, above this temperature the empirical fit becomes worse, and we are forced to use $Z > 2$ to properly represent the width. Note that with this slight modification to the formula, the parameters W_b and W_r keep the same meaning as the half-width at half-maximum on the blue and red sides, respectively. Above 300 °C, the spectrum amplitude near 400 nm is no longer well-represented by this modified formula and the blue tail is somewhat underestimated.

The following fit parameters of eq 2 reasonably describe the normalized hydrated electron spectra between 400 nm and the infrared cutoff in H_2O and D_2O up to 350 °C:

$$Z = 1.95 + 0.00129T$$

$$W_r = 0.281 + 3.65 \times 10^{-3}T - 5.14 \times 10^{-5}T^2 + 3.63 \times 10^{-7}T^3 - 1.18 \times 10^{-9}T^4 + 1.40 \times 10^{-12}T^5$$

$$E_{max} = 1.79 - 0.00250T + 2.54 \times 10^{-17}T^6 \qquad W_b = 0.51 \text{ in light water}$$

$$E_{max} = 1.84 - 0.00268T + 4.13 \times 10^{-17}T^6 \qquad W_b = 0.49 \text{ in heavy water}$$

where T is in °C. In Figure 5 the fitted parameters for light water are plotted vs temperature (symbols) as well as the polynomial fits above (smooth lines). Note that because the light water vibrational overtones cut off IR transmission, the Gaussian half-width cannot even be estimated in light water above 250 °C, so the fit to W_r for heavy water is assumed for both species and does give a reasonable fit to the light water data. In Figure 6 we plot the fitted parameters for heavy water (symbols) and polynomial fits to these parameters (smooth lines).

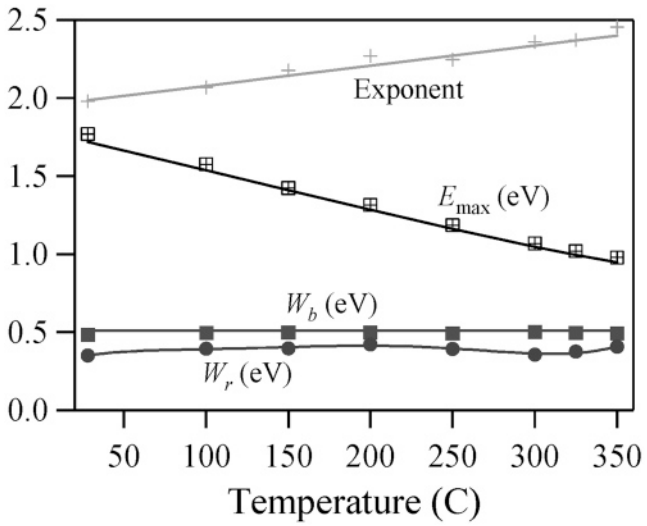

Figure 6. Fitting parameters (symbols) for heavy water solvated electron spectra, using the modified Gaussian−Lorentzian form described in the text. The pressure is 250 bar. The lines represent the smoothed values for the light water spectra, for comparison. There is no significant difference found in this study in the red side half-width W_r. The heavy water W_b half-width is slightly smaller and the E_{max} is slightly larger than the corresponding light water parameters.

We find that the red (Gaussian) half-width W_r is virtually identical in both H_2O and D_2O. The values of the parameters are in good agreement with earlier reports of Jou and Freeman[11] and of Christensen and Sehested.[39] Likewise our fitted E_{max} values agree with earlier work up to 200 °C. Christensen and Sehested[39] and more recently Wu et al.[10] reported a fairly sudden change in the temperature derivative of E_{max} above 200 °C, and a limiting value at about 1.2 eV. We also see a slight change in the slope, but it occurs closer to 300 °C, and the limiting value appears to be ca. 0.9 eV. We suspect that the spectra of previous workers were distorted by the photodiode secondary response problem.[33] However, the position defined as the maximum also depends strongly on the quality of the data in the wings and the functional form assumed for the spectrum shape.

The blue (Lorentzian) half-width W_b is virtually independent of temperature, as also observed by Jou and Freeman[11] (to 108 °C) and by Christensen and Sehested.[39] However, we agree with the values of Christensen and Sehested, just over 0.5 eV, rather

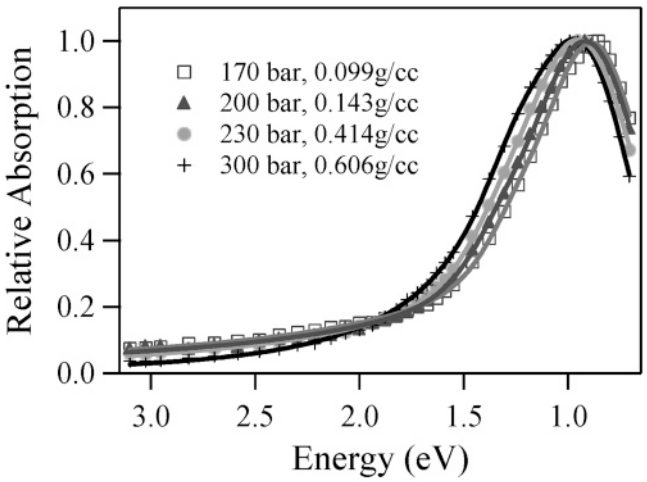

Figure 7. Normalized spectra of solvated electrons in heavy water at 375 °C, at different densities of the supercritical fluid. Relative amplitude of the blue tail increases as the density decreases.

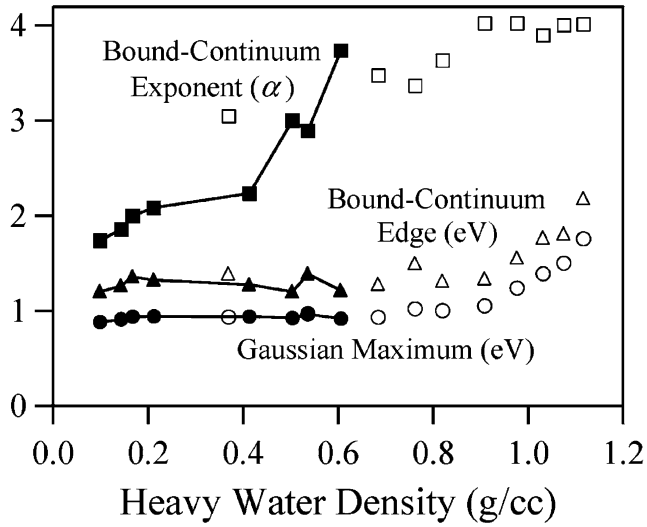

Figure 8. Selected fitting parameters for hydrated electron spectra vs density in heavy water, based on eq 3. Points connected by lines are all at 375 °C at various pressures. The other points correspond to different temperatures at 250 bar pressure.

than the lower values of Jou and Freeman around 0.45−0.48 eV. We suspect that the Jou and Freeman widths are too small because they used a photomultiplier detector with exponential drop off in quantum efficiency in the red. This means that the light actually being detected is heavily weighted toward the blue side of the monochromator band-pass. On the blue slope of the solvated electron spectrum, this implies the measured absorption will be smaller than it ought to be at the nominal center wavelength. Our photodiode detector does not have a large change in quantum efficiency with wavelength, and so this distortion will not be present.

In Figure 7, heavy water spectra are shown for several densities at 375 °C (reduced temperature of $T_r = 1.01$ in heavy water). Intermediate densities (near the critical density of 0.36 g/cc) are particularly difficult to obtain with good precision under supercritical conditions because of the great sensitivity of the fluid density to temperature and pressure fluctuations. A small red shift of the spectrum can be detected, and the relative amplitude of the blue tail increases as the density decreases. Still, there is relatively little change in the spectrum given the enormous density change in the water, suggesting that the inner solvation shell for the electrons is nearly constant.

Except at the highest density, these spectra cannot be fit with the modified Gaussian−Lorentzian form described above. The blue tail is far too large. To describe the spectra, we postulate a bound to bound transition with Gaussian line shape, and a bound to continuum tail which is just a power law $E^{-\alpha}$ of the energy. To "switch on" the bound to continuum transition, we multiply the power law (exponent $-\alpha$) by a sigmoidal function (cutoff parameters E_c and W_c). The overall expression is

$$\gamma(E) = B \exp(-[(E - E_{max})/W_r]^2 \ln(2)) + \frac{CE^{-\alpha}}{1 + \exp[(E_c - E)/W_c]} \quad (3)$$

where B and C are merely empirically fitted amplitude parameters. This function provides enough flexibility to fit/interpolate all of the spectra we have collected.

The spectra in both light and heavy water have been fit with this function, and the hope is to find a set of parameters that will tell us something meaningful about the changes in the electron solvation environment. W_r is identical to the Gaussian−Lorentzian fits shown above. The cutoff parameter W_c falls between 0.1 and 0.2 eV. Some of the parameters (E_{max}, E_c, and exponent α) required to fit the heavy water spectra are plotted vs density in Figure 8. The bound-continuum cutoff parameter E_c tracks E_{max}, roughly 0.3−0.4 eV higher in energy. The largest changes come in the exponent of the power law that describes the blue tail. Theory suggests that at sufficiently high photon energy this exponent should be 3.5 for an s-to-p symmetry bound-continuum transition, and the exponent should be larger than 2.5 for inverse second moments of the spectrum to converge.[25] Spectra for high-density water may all be fit with power law exponents in the 3−4 range, but the lower-density water spectra (below 0.4 g/cm^3) require exponents well below 2.5.

We conclude from this fitting exercise that we have not obtained line shape parameters any more meaningful than those from the empirical Gaussian−Lorentzian form. This is disappointing but is not a great surprise, because quantum molecular dynamics simulations of the hydrated electron suggest there should be three nondegenerate "s-to-p like" bound to bound transitions with different amplitudes,[15,17] in addition to the bound-continuum tail which need not look like a simple power law decay near the threshold energy.[25] Including all of these features of the simulation would require too many parameters for a unique fit. In the absence of a more rigorous description, the fit based on eq 3 is nevertheless useful for interpolation and integration. To avoid biasing any future fitting attempts by other workers, we present all of our normalized spectra in tabular form in Part A of the Supporting Information.

Moment Analysis. Once the line shapes are established, calculation of the moments $M(+1)$ and $M(-1)$ via eq 1 is straightforward. The absolute extinction coefficients are not needed because the unnormalized $M(\pm 1)$ integrals can be divided by the unnormalized $M(0)$ integral, which has the same arbitrary scale factor. The data, interpolated with the equations given above, contain most of the spectral information, but there still is missing information extending to zero frequency beyond the infrared and extending to infinite frequency beyond the ultraviolet. Assumptions must be made on the behavior of these wings of the spectrum. On the basis of the behavior of the red side of the heavy water spectrum up to 100 °C, a Gaussian function is an excellent representation even though it does not have the proper limiting value at zero. Therefore we carry out the integration using eq 3 down to a truncation energy of 0.2

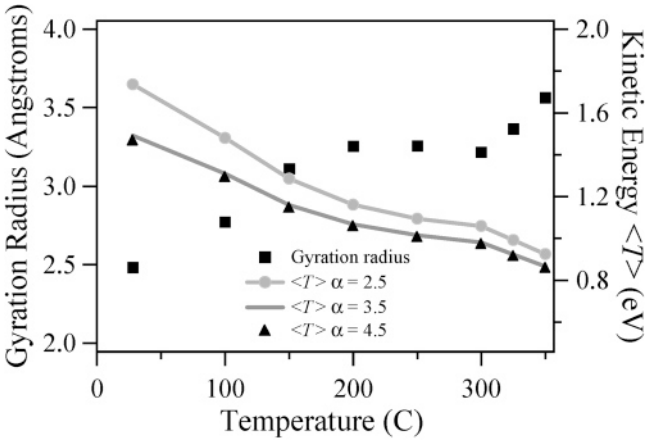

Figure 9. Temperature dependence of the average kinetic energy $\langle T \rangle$ and the gyration radius for the solvated electron in heavy water, as determined by analysis of the spectral moments. The pressure is 250 bar. The gyration radius is essentially independent of the assumption used for the extrapolation to infinite frequency. The kinetic energy is determined to within 10 or 20%. Note that points for $\alpha = 4.5$ lie nearly on top of the trace for $\alpha = 3.5$.

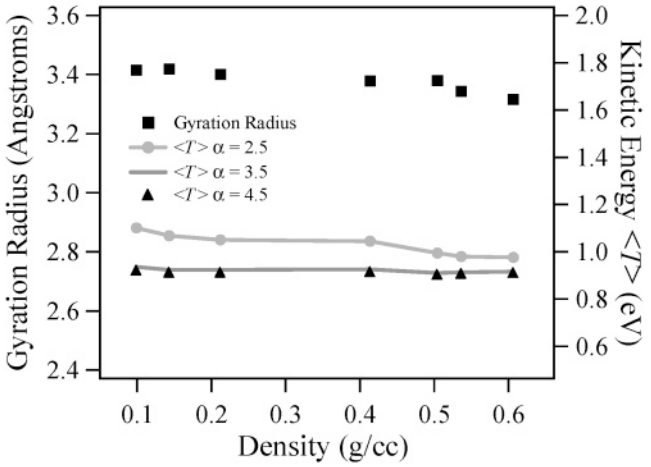

Figure 10. Radius of gyration and average kinetic energy for hydrated electrons in supercritical heavy water at 375 °C, as determined from the spectral moment analysis. Note that the points for $\alpha = 4.5$ lie nearly on top of the trace for $\alpha = 3.5$.

eV. On the blue side of the spectra, we have only collected data to 3.2 eV. We have used simple power law extensions of the spectra to integrate from 3.2 eV out to infinity. Several different values of the power law exponent $-\alpha$ were tried to investigate the sensitivity of the calculated moments to this approximation.

Figure 9 illustrates the temperature dependence of the average kinetic energy $\langle T \rangle$ and the average radius of gyration for the hydrated electron in heavy water. The symbols in Figure 9 for the power law extensions using exponents 4.5 and 3.5 are virtually superimposed, whereas using exponent 2.5 makes at most a 15% difference in the kinetic energy result. Virtually identical results (not shown) are obtained for the electron in light water. In Figure 10 we plot the same quantities as a function of the water density for the hydrated electron in supercritical heavy water at 375 °C. The average radius of gyration and kinetic energy of the electron hardly changes over the density range from 0.1 to 0.6 g/cm^3.

Solvation Thermodynamics. From the spectral moment analysis described above, we obtain parameters related to the energy of the solvated electron, and it will be interesting to compare these to the enthalpy and free energy of electron solvation. Shiraishi et al.[28] have experimentally derived the enthalpy and free energy for the equilibrium (I) up to 250 °C.

$$(e^-)_{aq} + H_2O \rightleftharpoons H + (OH^-)_{aq} \quad \text{(I)}$$

The conventional enthalpy and Gibbs energy of formation for both H_2O and $(OH^-)_{aq}$ are available from literature sources as a function of temperature and pressure. We have obtained smoothed values from the SUPCRT92 program,[36] which uses the modified HKF equation of state[40] to interpolate data up to 350 °C. We have also obtained the Gibbs energy and the enthalpy of formation for $(H_2)_{aq}$ from this source. The solvation properties of the H atom have been shown to be very similar to that of H_2.[41] Consequently, we can add the gas-phase enthalpy and Gibbs energy of formation of H atoms to the solvation energy of H_2, to obtain a good estimate of the aqueous H atom formation enthalpy and Gibbs energy. With these values in hand, we can calculate from the free energy and enthalpy of equilibrium (I), the conventional thermodynamic functions for formation of the hydrated electron ($(e^-)_{aq}$) as a function of temperature.

Conventional functions for the hydration process $(e^-)_g \rightarrow (e^-)_{aq}$ are obtained from the difference in liquid-phase and gas-phase thermodynamic functions ($X = H$, G, or S):

$$\Delta X_{hyd,conv} = \Delta X_{f,aq} - \Delta X_{f,gas} \quad (4)$$

These numbers are still of no value for comparison to the spectrum properties, because they are based on the arbitrary convention that the free energy and enthalpy of proton formation are zero at all temperatures. Essentially this means that the *absolute* hydration enthalpy or free energy is related to the conventional quantity by

$$\Delta X_{hyd,abs}(e^-) = \Delta X_{hyd,conv}(e^-) + (\Delta X_{hyd,abs}(H^+) + \Delta X_{f,gas}(H^+)) \quad (5)$$

To obtain the desired absolute properties for the electron requires that we find absolute solvation properties for the proton, $\Delta X_{hyd,abs}(H^+)$.

The search for a way to determine these quantities for the proton has a long history. The problem stems from the fact that solution-phase measurements are always performed on electrically neutral systems, so that only the *sum* of positive and negative ion properties can be measured. It is necessary, for at least one pair of ions, to obtain information on the *difference* in hydration energies. Tissandier et al.[29] have recently shown how this difference quantity can be extracted from a comparison of ionic cluster stepwise hydration data, and the conventional free energies and enthalpies for aqueous ions (i.e., extrapolation to the infinite cluster). The enthalpy of hydration determined by this method is about 40−50 kJ/mol more negative than most previous estimates. Coe further showed how a minimal calculation can be made just using energetics of the first hydration reaction of a set of monatomic ions with one water molecule.[12] This can easily be accomplished with sufficient precision using B3LYP density functional calculations on a personal computer.

We have carried out this calculation to obtain the absolute proton hydration thermodynamic properties as a function of temperature at different pressures. A complete description of the analysis and results will be given elsewhere.[31] In part B of the Supporting Information, we provide tables of the data input required to execute the method of Tissandier et al.[29] and Coe[12] for the range of temperature up to 350 °C along the liquid−vapor coexistence curve. Then, using the conventional free

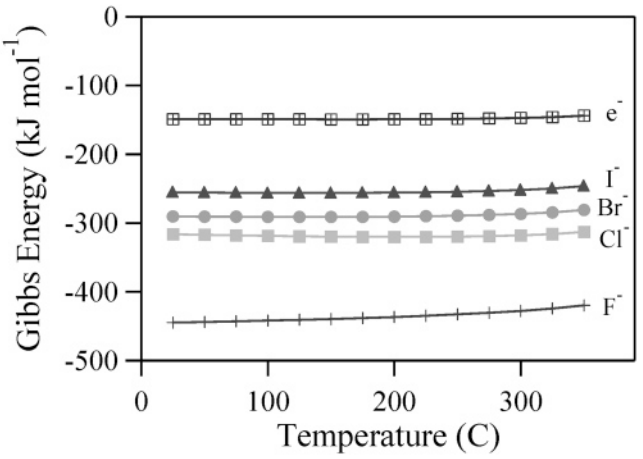

Figure 11. Absolute Gibbs free energy of hydration of the electron and several other monatomic anions, calculated along the liquid−vapor coexistence curve.

energy of hydration for electrons given by Shiraishi et al.,[28] we can also obtain the absolute Gibbs energy of hydration. To use this result in the Born theory of ion hydration, we use the same standard state concentration in both liquid and gas phase, to remove the density dependence of the entropy.[42] The results for the electron are plotted up to 350 °C in Figure 11, along with absolute solvation free energy of other monatomic anions.[43] We should caution that in Figure 11 we have extrapolated the formulas provided by Shiraishi to 350 °C, even though data were only collected to 250 °C. Our preliminary investigation of kinetics at the higher temperature suggests that the extrapolation for the critical equilibrium constant is not far off at 300 °C. The curves for classical ions in Figure 11 are based on interpolation of measured data as obtained from SUPCRT92.

Discussion

The origin of the strong temperature dependence of the hydrated electron spectrum has gone unexplained for many years. Several simulation attempts failed to reproduce the experimental result. In a recent simulation of the hydrated electron at temperatures up to the supercritical regime, Nicolas et al.[15] claim to explain the temperature effect—not as a temperature effect, but as a change in density of the water. Their simulation showed virtually no change in E_{max} between 25 and 250 °C, when the density was kept at 1 g/cc, or between 250 and 375 °C when the density was 0.6 g/cc. But when the density was allowed to change, the very large red shift was recovered. A very recent first principles Car−Parrinello MD simulation[13] compared room-temperature water conditions with supercritical water of density 0.73 g/cm^3. A red shift was found, but because both density and temperature were changed, no strong statement can be made. It was found that the average number of water molecules in the first shell decreased from about six to about four under supercritical conditions.[13] Laria and Skaf[14] have reported path-integral MD studies of the hydrated electron as a function of supercritical water density in the range 1.0 to 0.05 g/cm^3. A large increase in electron gyration radius was found as a function of decreasing water density, especially below 0.1 g/cc where the electron essentially "desolvated."

Our data in supercritical water would seem to be at variance with most of these simulation results. The E_{max} of heavy water spectra in Figure 7 change only slightly between 0.6 and 0.1 g/cc, and the corresponding radius of gyration in Figure 9 does not change much at all. Thus there is little spectrum shift or change in radius for a factor of 6 change in density. This directly contradicts the result of Laria and Skaf.[14] Nicolas et al.[15] only reported simulation results for densities greater or equal to 0.46 g/cc. However a very significant spectrum shift of over 0.2 eV was still reported between 300 °C, 0.63 g/cc and 400 °C, 0.46 g/cc and ascribed to the density change.

Given the insights from simulation and the results of our experiments, we suggest the following global picture for the electron solvation by water: At densities below 0.5 g/cm^3 (and above 0.1 g/cm^3) the electron attracts (perhaps four) solvating water molecules to an optimum distance, such that the radius of gyration is about 3.4 Å. The electron absorbs in the infrared with an E_{max} value near 1.0 eV. At higher water densities, the water molecules begin to squeeze the electron wave function, reducing the radius of gyration and forcing a blue shift of the spectrum. However, it is not clear that there is no temperature effect on the spectrum or wave function if the density is kept constant above 0.5 g/cc. A test of this assertion can be obtained from existing experiments on the pressure dependence of E_{max} near room temperature, because it should not matter if the density is changed via temperature or pressure. Jou and Freeman[44] measured the pressure-dependent blue shift of the spectrum at 27 °C up to 2000 kbar. When converted to a density derivative, the blue shift amounts to 0.0049 eV/(kg/m^3). When similarly converted into a density change, the temperature derivative of the spectrum near 27 °C amounts to 0.0017 eV/(kg/m^3).[11] Moreover, the E_{max} is quite a linear function of temperature between −4 and +100 °C, but the water density is not. Michael et al.[45] report a spectrum at −4 °C in supercooled water that is blue shifted relative to higher temperature, even though the bulk density is decreased. All of these comparisons illustrate that although density is a very important component of the spectral shift, temperature nevertheless plays another role as well. Perhaps this involves changes to the hydrogen bonding network and the connections to the water of the inner hydration shell. The strong interactions of the electron with the inner hydration shell are only crudely represented by partial charges and simple coulomb potentials in most simulations.

We do observe a change in the relative amplitude of the blue tail and the maximum absorption when we go to the low end of our density range in Figure 7. Virtually all simulations of the hydrated electron,[15−17] supported by recent Raman observations[46−49] and ultrafast kinetics experiments,[18,20,21] suggest that the hydrated electron spectrum consists primarily of three strongly allowed bound to bound, s-to-p-like subbands. The asymmetry in the spectrum is attributed primarily to the nondegeneracy of the three subbands, but the highest energy subband is also presumed to overlap with the onset of bound to continuum transitions that are responsible for the blue tail. The change in spectrum shape in low-density supercritical water suggests that the bound to continuum absorption gains more oscillator strength in this regime. One can only speculate that this results from fewer water molecules in the electron's solvation shell. It will be interesting to record hydrated electron spectra at even lower densities to examine this trend in the future.

The application of the moment analysis to the spectra has given data on both the size and the kinetic energy of the electron. The classical Born theory for ion solvation also relates the ion radius (r) and the free energy of ionic hydration (ΔG_{hyd}), via the equation (in atomic units):

$$\Delta G_{hyd} = \frac{1}{2r}\left(\frac{1}{\epsilon} - 1\right) \qquad (6)$$

where ϵ is the solvent dielectric constant. A comparison of Born radius and the electron radius of gyration would therefore seem

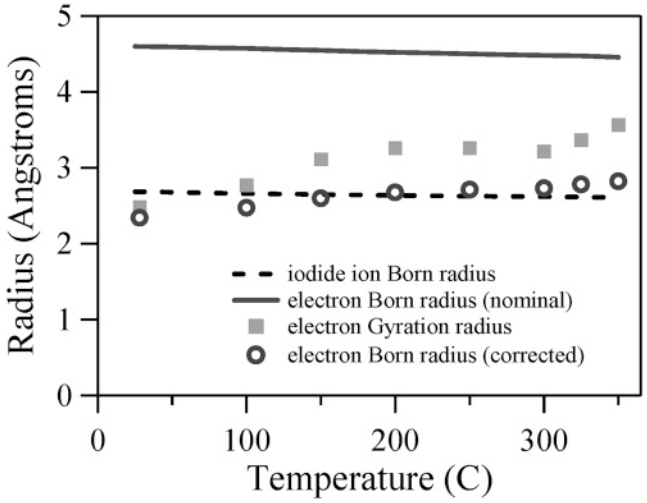

Figure 12. Nominal Born radii for the iodide ion and the electron calculated from the absolute Gibbs energy of hydration and a corrected Born radius obtained by first subtracting the electron kinetic energy. The corrected Born radius at least qualitatively resembles the gyration radius obtained from moment analysis of the spectrum.

to be instructive. In fact, one might expect that the free energy or enthalpy of hydration could be extrapolated from the spectrum.

Given the large change in electron gyration radius implied by the spectrum, on the basis of eq 6 we expected a large change in the electron hydration energy. The absolute free energy of electron hydration is plotted in Figure 11. It is remarkably insensitive to temperature and qualitatively resembles the hydration free energy of the other monatomic ions plotted. The electron free energy is least negative of these ions, and so one expects it must be the "largest." The nominal Born radius for the electron and the nominal Born radius for the iodide ion (for comparison) are both plotted in Figure 12 as a function of temperature, along with the radius of gyration from moment analysis of the spectrum. There is no qualitative resemblance of the two determinations of the electron radius.

At this point we began to reconsider the assumptions of the Born theory, which is based on classical electrostatics for the charging of a sphere in a dielectric continuum. Nowhere in the Born theory is quantum zero point energy considered. In the electron solvation process, a major part of the work involves localizing the electron into a small volume, thereby increasing the electron kinetic energy. A proper thermodynamic cycle for the quantum particle could be constructed by first localizing the particle within the sphere of radius r, and then charging the sphere in the dielectric medium as done in the Born theory. Neglecting the small entropy contribution of electron localization[50] (ca. 6 kJ mol^{-1} at 300 K), a corrected Born theory expression would be

$$\Delta G_{\mathrm{hyd}} - \langle T \rangle = \frac{1}{2r}\left(\frac{1}{\epsilon} - 1\right) \qquad (7)$$

From the spectral moment analysis, we have a measurement of the average electron kinetic energy, which is in the range 100−200 kJ/mol and depends on the temperature. A simple correction can therefore be made, by subtracting the electron kinetic energy from the free energy of hydration. This "classical" free energy can then be used in the Born equation to estimate a "corrected" Born radius. This quantity is also plotted in Figure 12 as the open circles. With this correction made, we have a qualitatively correct behavior of the electron's radius, showing an increase with temperature.

At room temperature, the radius of gyration and corrected Born radius nearly coincide, but at higher temperature the radius of gyration is larger than the effective Born radius. Several studies suggest that the Born radius of a classical ion should be interpreted essentially as the radius of the first peak in the ion−oxygen radial distribution function $g(r)$.[51,52] Several simulation studies for the hydrated electron find this first (small) peak in $g(r)$ at a somewhat larger value than the radius of gyration,[15,17] so one might expect that the corrected Born radius in Figure 12 should be slightly larger than the radius of gyration. Nevertheless, the overall agreement between the two experimental radii is very good, and we can have some confidence that the assumptions made in both the Born theory analysis and the spectral moment analysis are reasonable.

Summary

We have carried out careful measurements of the hydrated electron absorption spectrum in both light and heavy water between 400 and 1700 nm, and up to 400 °C. At 375 °C in heavy water, the density was changed between 0.6 and 0.1 g/cm^3. Fitting parameters are reported to allow estimates of the spectrum amplitude under all of these conditions. As reported in the past, the spectrum appears to be Gaussian on the red side but Lorentzian on the blue side, below 100 °C at 1 atm pressure. At higher temperatures, deviations from this empirical form become apparent. In supercritical water at 0.5 g/cc and below, Gaussian−Lorentzian is a very bad description. Instead we fit to a sum of bound-bound Gaussian and bound-continuum power law functions.

The spectrum is integrated to obtain information on the electron kinetic energy and the radius of gyration. There is little effect of water density on these quantities in supercritical water, in contradiction to some recent simulation predictions. We have used literature data to calculate the free energy of hydration for electrons as a function of temperature up to 250 °C. Surprisingly, the Gibbs energy of hydration is insensitive to temperature. We show that by subtracting the electron kinetic energy from the Gibbs energy, we can calculate an effective Born radius that is qualitatively consistent with the spectral moment theory radius of gyration.

Acknowledgment. We thank Dr. Sergey Chemerisov for maintaining the electron accelerator used in this work. We are greatly indebted to Prof. James Coe of Ohio State University for consultations and calculations on the absolute proton hydration thermodynamics. Finally, we thank Dr. Peter Rossky for discussions on the quantum correction to the Born theory expression. Work at Notre Dame Radiation Laboratory and at Argonne National Laboratory (contract number W-31-109-ENG-38) was performed under the auspices of the Office of Science, Division of Chemical Science, US-DOE. Additional funding for K. Takahashi, J. A. Cline, and T. W. Marin was provided by US-DOE Nuclear Energy Research Initiative grants M9SF99-0276 and M2SF02-0060. This is document number NDRL-4566 from the Notre Dame Radiation Laboratory.

Supporting Information Available: (A) Normalized spectra for hydrated electrons in both light and heavy water, in tabular form. (B) Tables of the data used to calculate absolute proton and electron hydration free energy, and a brief description of the procedure used. This material is available free of charge via the Internet at http://pubs.acs.org.

References and Notes

(1) Savage, P. E.; Gopalan, S.; Mizan, T. I.; Martino, C. J.; Brock, E. E. *AIChE J.* **1995**, *41*, 1723.

(2) Savage, P. E. *Chem. Rev.* **1999**, *99*, 603.
(3) Akiya, N.; Savage, P. E. *Chem. Rev.* **2002**, *102*, 2725.
(4) Elliot, A. J. Rate Constants and G-Values for the Simulation of the Radiolysis of Light Water over the Range 0−300 °C. Atomic Energy of Canada, Ltd.: Chalk River, Ontario, Canada, 1994.
(5) Elliot, A. J.; Ouellette, D. C.; Stuart, C. R. The Temperature Dependence of the Rate Constants and Yields for the Simulation of the Radiolysis of Heavy Water. Atomic Energy of Canada, Ltd.: Chalk River, Ontario, Canada, 1996.
(6) McCracken, D. R.; Tsang, K. T.; Laughton, P. J. Aspects of the physics and chemistry of Water Radiolysis by Fast Neutrons and Fast Electrons in Nuclear Reactors. Atomic Energy of Canada, Ltd.: Chalk River, Ontario, Canada, 1998.
(7) Cline, J. A.; Takahashi, K.; Marin, T. W.; Jonah, C. D.; Bartels, D. M. *J. Phys. Chem. A* **2002**, *106*, 12260.
(8) Marin, T. W.; Cline, J. A.; Bartels, D. M.; Jonah, C. D.; Takahashi, K. *J. Phys. Chem. A* **2002**, *106*, 12280.
(9) Hart, E. J.; Anbar, M. *The Hydrated Electron*; Wiley-Interscience: New York, 1970.
(10) Wu, G.; Katsumura, Y.; Muroya, Y.; Li, X.; Terada, Y. *Chem. Phys. Lett.* **2000**, *325*, 531.
(11) Jou, F.-Y.; Freeman, G. R. *J. Phys. Chem.* **1979**, *83*, 2383.
(12) Coe, J. V. *Int. Rev. Phys. Chem.* **2001**, *20*, 33.
(13) Boero, M.; Parrinello, M.; Terakura, K.; Ikeshoji, T.; Liew, C. C. *Phys. Rev. Lett.* **2003**, *90*.
(14) Laria, D.; Skaf, M. S. *J. Phys. Chem. A* **2002**, *106*, 8066.
(15) Nicolas, C.; Boutin, A.; Levy, B.; Borgis, D. *J. Chem. Phys.* **2003**, *118*, 9689.
(16) Romero, C.; Jonah, C. D. *J. Chem. Phys.* **1989**, *90*, 1877.
(17) Rossky, P. J.; Schnitker, J. *J. Phys. Chem.* **1988**, *92*, 4277.
(18) Kambhampati, P.; Son, D. H.; Kee, T. W.; Barbara, P. F. *J. Phys. Chem. A* **2002**, *106*, 2374.
(19) Kee, T. W.; Son, D. H.; Kambhampati, P.; Barbara, P. F. *J. Phys. Chem. A* **2001**, *105*, 8434.
(20) Son, D. H.; Kambhampati, P.; Kee, T. W.; Barbara, P. F. *J. Phys. Chem. A* **2001**, *105*, 8269.
(21) Son, D. H.; Kambhampati, P.; Kee, T. W.; Barbara, P. F. *Chem. Phys. Lett.* **2001**, *342*, 571.
(22) Bartels, D. M. *J. Chem. Phys.* **2001**, *115*, 4404.
(23) Brodskii, A. M.; Tsarevskii, A. V. *Sov. Phys. JETP* **1976**, *43*, 111.
(24) Carmichael, I. *J. Phys. Chem.* **1980**, *84*, 1076.
(25) Golden, S.; Tuttle, T. R., Jr. *J. Chem. Soc., Faraday Trans. 2* **1979**, *75*, 474.
(26) Tuttle, T. R., Jr.; Golden, S. *J. Phys. Chem.* **1991**, *95*, 5725.
(27) Marbach, W.; Asaad, A. N.; Krebs, P. *J. Phys. Chem. A* **1999**, *103*, 28.
(28) Shiraishi, H.; Sunaryo, G. R.; Ishigure, K. *J. Phys. Chem.* **1994**, *98*, 5164.
(29) Tissandier, M. D.; Cowen, K. A.; Feng, W. Y.; Gundlach, E.; Cohen, M. H.; Earhart, A. D.; Tuttle, T. R.; Coe, J. V. *J. Phys. Chem. A* **1998**, *102*, 9308.
(30) Tuttle, T. R.; Malaxos, S.; Coe, J. V. *J. Phys. Chem. A* **2002**, *106*, 925.
(31) Bartels, D. M.; Coe, J. V. *J. Am. Chem. Soc.,* manuscript in preparation.
(32) Takahashi, K.; Cline, J. A.; Bartels, D. M.; Jonah, C. D. *Rev. Sci. Instrum.* **2000**, *71*, 3345.
(33) Cline, J. A.; Jonah, C. D.; Bartels, D. M. *Rev. Sci. Instr.* **2002**, *73*, 3908.
(34) Sehested, K.; Christensen, H. *Rad. Phys. Chem.* **1990**, *36*, 499.
(35) Wagner; Kruse. *Properties of Water and Steam*; Springer, 1997.
(36) Johnson, J. W.; Oelkers, E. H.; Helgeson., H. C. *Comput. Geosci.* **1992**, *18*, 899.
(37) Uematsu, M.; Franck, E. U. *J. Phys. Chem. Ref. Data* **1980**, *9*, 1291.
(38) Hill, P. G.; MacMillan, R. D.; Lee, V. Tables of Thermodynamic Properties of Heavy Water in SI Units. Atomic Energy of Canada, Ltd.: Missisauga, Ontario, Canada, 1981.
(39) Christensen, H.; Sehested, K. *J. Phys. Chem.* **1986**, *90*, 186.
(40) J. C. Tanger, I.; Helgeson, H. C. *Am. J. Sci.* **1988**, *288*.
(41) Roduner, E.; Bartels, D. M. *Ber. Bunsen-Ges. Phys. Chem.* **1992**, *96*, 1037.
(42) Ben-Naim, A. *Solvation Thermodynamics*; Plenum Press: New York, 1987.
(43) Asthagiri et al. (Asthagiri, D.; Pratt, L. R.; Ashbaugh, H. S. *J. Chem. Phys.* **2003**, *119*, 2702) contend that the quantity actually measured in the cluster-based work of Tissandier et al. includes the "potential of the phase" that is present due to electroneutrality requirements. They suggest this quantity is negative and of magnitude over 40 kJ mol^{-1}. If this is correct, the numbers for anions that we report in Figure 11 should be more negative by this amount.
(44) Jou, F.-Y.; Freeman, G. R. *J. Phys. Chem.* **1977**, *81*, 909.
(45) Michael, B. D.; Hart, E. J.; Schmidt, K. H. *J. Phys. Chem.* **1971**, *75*, 2798.
(46) Tauber, M. J.; Mathies, R. A. *J. Phys. Chem. A* **2001**, *105*, 10952.
(47) Tauber, M. J.; Mathies, R. A. *J. Am. Chem. Soc.* **2003**, *125*, 1394.
(48) Mizuno, M.; Tahara, T. *J. Phys. Chem. A* **2003**, *107*, 2411.
(49) Tauber, M. J.; Mathies, R. A. *Chem. Phys. Lett.* **2002**, *354*, 518.
(50) Han, P.; Bartels, D. M. *J. Phys. Chem.* **1991**, *95*, 5367.
(51) Schmid, R.; Miah, A. M.; Sapunov, V. N. *Phys. Chem. Chem. Phys.* **2000**, *2*, 97.
(52) Roux, B.; Yu, H.-A.; Karplus, M. *J. Phys. Chem.* **1990**, *94*, 4683.